

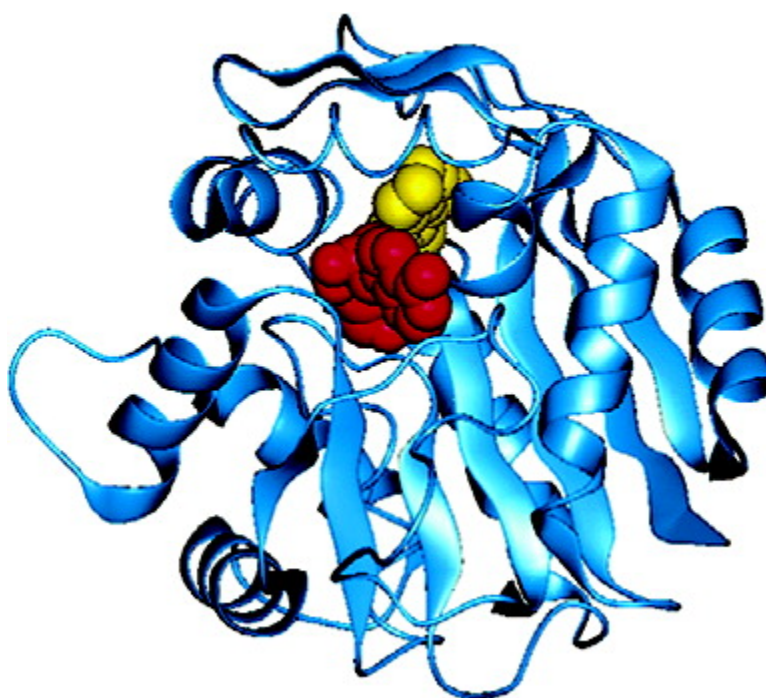
Article

Structural, Mutagenic, and Kinetic Analysis of the Binding of Substrates and Inhibitors of Human Phenylethanolamine *N*-Methyltransferase

Qian Wu, Christine L. Gee, Frank Lin, Joel D. Tyndall,
Jennifer L. Martin, Gary L. Grunewald, and Michael J. McLeish

J. Med. Chem., **2005**, 48 (23), 7243-7252 • DOI: 10.1021/jm050568o • Publication Date (Web): 14 October 2005

Downloaded from <http://pubs.acs.org> on March 29, 2009



More About This Article

Additional resources and features associated with this article are available within the HTML version:

- Supporting Information
- Links to the 1 articles that cite this article, as of the time of this article download
- Access to high resolution figures
- Links to articles and content related to this article
- Copyright permission to reproduce figures and/or text from this article



ACS Publications
High quality. High impact.

Journal of
Medicinal Chemistry

Subscriber access provided by American Chemical Society

[View the Full Text HTML](#)



ACS Publications
High quality. High impact.

Journal of Medicinal Chemistry is published by the American Chemical Society, 1155
Sixteenth Street N.W., Washington, DC 20036

Structural, Mutagenic, and Kinetic Analysis of the Binding of Substrates and Inhibitors of Human Phenylethanolamine *N*-Methyltransferase

Qian Wu,[‡] Christine L. Gee,[§] Frank Lin,[§] Joel D. Tyndall,^{§,‡} Jennifer L. Martin,[§] Gary L. Grunewald,[‡] and Michael J. McLeish^{*,‡}

Department of Medicinal Chemistry, University of Michigan, 428 Church Street, Ann Arbor, Michigan 48109, Institute for Molecular Bioscience and ARC Special Research Centre for Functional and Applied Genomics, University of Queensland, Brisbane QLD 4072, Australia, and Department of Medicinal Chemistry, University of Kansas, 1251 Wescoe Hall Drive, Lawrence, Kansas 66045

Received June 16, 2005

The X-ray structure of human phenylethanolamine *N*-methyltransferase (hPNMT) complexed with its product, *S*-adenosyl-L-homocysteine (**4**), and the most potent inhibitor reported to date, SK&F 64139 (**7**), was used to identify the residues involved in inhibitor binding. Four of these residues, Val53, Lys57, Glu219 and Asp267, were replaced, in turn, with alanine. All variants had increased K_m values for phenylethanolamine (**10**), but only D267A showed a noteworthy (20-fold) decrease in its k_{cat} value. Both WT hPNMT and D267A had similar k_{cat} values for a rigid analogue, *anti*-9-amino-6-(trifluoromethyl)benzonorborene (**12**), suggesting that Asp267 plays an important role in positioning the substrate but does not participate directly in catalysis. The K_i values for the binding of inhibitors such as **7** to the E219A and D267A variants increased by 2–3 orders of magnitude. Further, the inhibitors were shown to bind up to 50-fold more tightly in the presence of *S*-adenosyl-L-methionine (**3**), suggesting that the binding of the latter brings about a conformational change in the enzyme.

Phenylethanolamine *N*-methyltransferase (PNMT; EC 2.1.1.28) catalyzes the terminal step in catecholamine biosynthesis, i.e., the conversion of norepinephrine (**1**) to epinephrine (**2**, Figure 1) with the concomitant conversion of *S*-adenosyl-L-methionine (AdoMet, **3**) to *S*-adenosyl-L-homocysteine (AdoHcy, **4**).^{1,2} Although epinephrine (Epi, **2**) makes up 5–10% of the total catecholamine content of the brain,^{2,3} its function within the central nervous system (CNS) is not well understood.⁴ Over the years it has been implicated in activities ranging from central control of blood pressure⁵ and respiration,^{6,7} to the secretion of hormones from the pituitary.⁸ It may even be responsible for some of the neurodegeneration found in Alzheimer's disease.^{9,10} It is conceivable that an inhibitor of PNMT could be used to regulate levels of **2** within the CNS, thus providing considerable assistance in elucidating the role(s) of central Epi (**2**).

Shortly after the isolation of PNMT it was recognized that phenylethylamines and amphetamines were able to competitively inhibit PNMT^{11–13} and that potency could be greatly enhanced by the addition of chlorine substituents to the aromatic ring.¹³ Later benzylamines were also shown to be competitive inhibitors of PNMT, with activity being increased not only by halogen substituents on the aromatic ring, but also by the addition of an α -methyl group.¹⁴ The benzylamines, such as 2,3-dichloro- α -methylbenzylamine (**5**, Figure 2), generally were more potent than the amphetamines, ex-

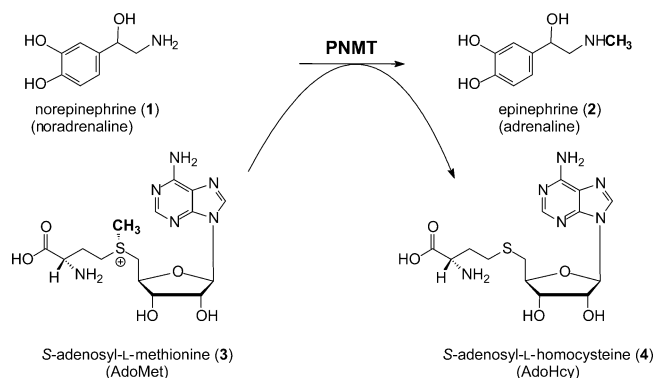


Figure 1. PNMT catalyzes the transfer of an activated methyl group from *S*-adenosyl-L-methionine (**3**) to the amine of norepinephrine (**1**) forming epinephrine (**2**) and *S*-adenosyl-L-homocysteine (**4**).

emplified by 3,4-dichloroamphetamine (**6**, Figure 2), and were the first to be used as inhibitors of catecholamine biosynthesis *in vivo*.¹⁵ Constraining the aminoethyl side chain of β -phenylethylamine into a fused ring system also resulted in increased PNMT-inhibitory activity *in vitro*.¹⁶ This led to the development of the 1,2,3,4-tetrahydroisoquinoline (THIQ) derivatives, SK&F 64139 (**7**)^{16,17} and SK&F 29661 (**8**),¹⁸ and as well as the 2,3,4,5-tetrahydro-1*H*-2-benzazepine (THBA) derivative, LY134046 (**9**, Figure 2).¹⁹ Both **7**²⁰ and **9**¹⁹ proved to be effective *in vivo* inhibitors of adrenal and CNS PNMT, but, *in vivo*, **8** only inhibited the adrenal enzyme.¹⁸

Many of the PNMT inhibitors that are sufficiently lipophilic to cross the blood–brain barrier, such as **7** and **9**, have been found to interact with other biologically important sites, such as the α_2 -adrenoceptors, thereby limiting their utility as pharmacological tools.^{17,19} While **8** is selective for PNMT, there are varying reports

* To whom correspondence should be addressed. Tel: (734) 615 1787; Fax: (734) 615 3079. E-mail: mcleish@umich.edu.

[‡] University of Michigan.

[§] University of Queensland.

[‡] University of Kansas.

[‡] Present address: National School of Pharmacy, University of Otago, Dunedin, New Zealand, 9015.

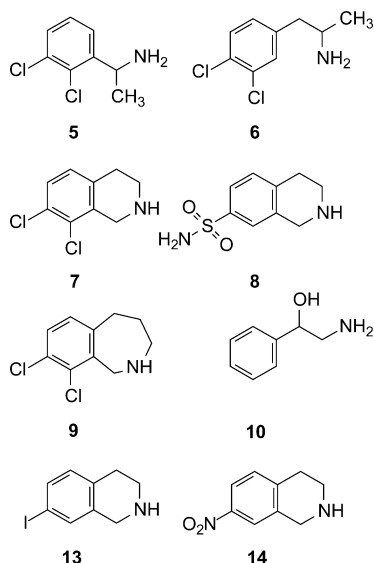


Figure 2. Structures of PNMT substrates and inhibitors described in the text.

about its ability to cross the blood–brain barrier.^{18,21,22} The most recent evidence suggests that it cannot, which would also render it ineffective as a pharmacological tool.²² Initially, molecular modeling techniques were employed to design more potent and selective PNMT inhibitors with testing being carried out against the bovine enzyme.^{23,24} Subsequent crystallographic studies, facilitated by the expression and purification of human PNMT (hPNMT) from *Escherichia coli*,²⁵ resulted in the solution of the X-ray structure of hPNMT cocrystallized with **4** and several inhibitors.^{26,27}

The X-ray structures show that the active site is covered, rather like that of several AdoMet-dependent small molecule methyltransferases such as glycine,²⁸ histamine,²⁹ and guanidinoacetate³⁰ *N*-methyltransferases. Although it is clear that a significant conformational change is required to make the active site accessible for the binding of substrates and/or inhibitors, the hPNMT structures could be used to model the binding of **1** in the active site.²⁶ The model suggested that many of the residues interacting with the inhibitors are also likely to be involved in substrate binding and that, as predicted by earlier structure–activity studies,³¹ the β -hydroxyl group of the substrate is likely to occupy the same region in space as the aliphatic nitrogen of THIQ or THBA-type inhibitors.

Although there have been considerable advances in the development of potent and highly selective inhibitors of hPNMT that are predicted to cross the blood–brain barrier,^{32,33} the enzyme itself has undergone very little structural or mechanistic analysis. Here we describe the crystal structure of hPNMT complexed with the reaction product, **4**, and the potent THIQ inhibitor, **7**. By comparison with the binding of the THBA derivative, **9**, we identified several residues at the active site that are expected to be important in substrate and inhibitor binding. These were mutated and subjected to kinetic analysis.

Results and Discussion

Comparison of the Binding of **7 and **9** to hPNMT.** Derivatives containing either a THIQ or a THBA

Table 1. X-ray Data and Refinement Statistics for hPNMT:4:7 Complex

hPNMT:4:7	
space group	<i>P</i> 4 ₃ 2 ₁ 2
unit cell (Å)	
<i>a</i> , <i>b</i>	93.9
<i>c</i>	188.3
α , β , γ	90
observations	234499
unique reflections	33827
resoln range (Å) (top shell)	33.25–2.4 (2.49–2.4)
<i>I</i> / σ (<i>I</i>)	10.5 (3.3)
completeness (%)	100 (100)
<i>R</i> _{merge} (%)	7.8 (43.1)
Refinement	
reflns ($ F > 0$) of working set (test set)	30372 (3362)
<i>R</i> _{cryst} / <i>R</i> _{free}	21.3/24.3
no. non-hydrogen atoms	
protein and ligands	4226
water	207
rmsd from ideal geometry	0.006
bond length (Å)	1.32
bond angle (deg)	
Ramachandran	
% in most favored region	90
% in disallowed region	0.2

nucleus (Figure 2) have proved to be effective inhibitors of PNMT.^{16–19} Compounds **7** and **9** are THIQ and THBA inhibitors, respectively, both of which have two chloro substituents on the aromatic ring and both are able to cross the blood–brain barrier to inhibit the CNS enzyme. They differ only in the size of the fused aliphatic ring. Comparison of the binding of **7** and **9** in the hPNMT active site will be useful in examining the effect of the different fused ring structures on molecular recognition by hPNMT. The structure of the hPNMT·**4**·**9** complex has recently been published,²⁷ and we have now determined the structure of the hPNMT·**4**·**7** complex. Crystals of this complex were found to be isomorphous with those of the previously determined structures.^{26,27} The hPNMT·**4**·**7** structure was solved by difference Fourier methods and refined at 2.4 Å resolution with excellent statistics (Table 1). Figure 3 shows the binding of (A) **7**, (B) **8**, and (C) **9** in the hPNMT·**4** complex. The aromatic ring of each inhibitor slots into a narrow cleft between the side chains of Asn39 and Phe182^{26,27} with further positioning being mediated by interactions with several recognition residues. Table 2 provides a more detailed summary of the individual binding interactions between four of these residues, Val53, Lys57, Glu219, and Asp267, and the three inhibitors. These results show that, when compared with **7** (Figure 3D), the larger pucker of the fused ring of **9** leads to a different recognition of their amines. First, the positions of the nitrogens of the two inhibitors are separated by 1.3–1.5 Å in the active site. Second, the ring nitrogen of **7** (and other THIQ inhibitors)²⁷ interacts directly with Glu219 and indirectly with Asp267, whereas the nitrogen of the THBA inhibitor, **9**, interacts directly with Asp267 (displacing a bridging water molecule) and via a considerably longer interaction with Glu219 (3.1–3.8 Å). The fused ring systems of the two are separated by 0.6–1.0 Å in the active site, but this does not translate to a significantly different recognition of the halogen substituents on the aromatic rings. Both halogens on **7** and **9** make similar van der Waals interactions with Val53 and Lys57, which is

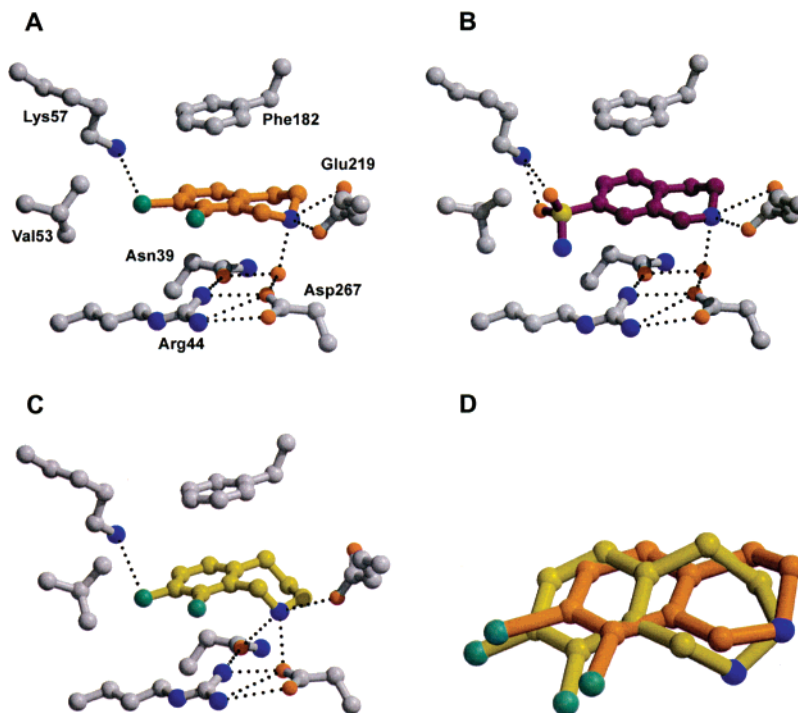


Figure 3. Comparison of THIQ and THBA inhibitor binding to PNMT. Binding mode of (A) **7** in orange (B) **8** in purple, and (C) **9** in yellow after superimposition of the enzyme structures, showing hydrogen bond interactions and orientations of active site residues described in the text. The amine-interacting water from the cocrystal structures with **7** and **8** are shown. (D) Superimposition of the bound conformations and orientations of the THIQ inhibitor **7** and THBA inhibitor **9**. The figure was generated using Molscript v2.0.1⁶² and Raster3D V2.7c.⁶³

Table 2. Distances of HPNMT Contacts^a with (A) **7**, (B) **8**, and (C) **9**

hPNMT interacting atom	(A) 7 ^b		(B) 8 ^c		(C) 9 ^d	
	ligand atom	distance (Å)	ligand atom	distance (Å)	ligand atom	distance (Å)
Val53 CG1	7-Cl	3.7	O2	3.2	8-Cl	3.2
			O1	5.0	9-Cl	4.5
			N'	4.1–4.7		
Val53 CG2	7-Cl	3.5–4.5	O2	4.0	8-Cl	3.8
			O1	4.6	9-Cl	5.0
			N'	3.7		
Lys57 NZ	7-Cl	3.6	O1	2.6	8-Cl	3.9
			O2	3.3		
E219 OE1	N1	2.9	N1	2.8	N1	3.1–3.8
E219 OE2	N1	3.5	N1	3.3		
D267 OD2	N1	3.6	N1	3.4	N1	2.6
Wat OH2	N1	2.7	N1	2.8		

^a Cutoffs used are 4 Å for possible hydrogen bond interactions and 5.0 Å for van der Waals interactions. Values are an average of the measurements for the two PNMT complexes in the asymmetric unit of the crystal structure, or given as a range if the values differ by more than 0.3 Å. ^b Data from this work, solved at 2.4 Å resolution. ^c Obtained using coordinates from PDB 1HNN²⁶ solved at 2.4 Å resolution. ^d Obtained using coordinates from PDB 1N7I²⁷ solved at 2.8 Å resolution.

consistent with earlier results²⁷ suggesting that the enzyme accommodates structural and chemical differences in the aromatic substituents of the inhibitors by making conformational adjustments to Val53 and Lys57. In addition, these results show that, small differences notwithstanding, THIQ inhibitors with hydrophobic substituents such as **7** and **13** bind in the same mode as the hydrophilic inhibitor, **8**. On the basis of QSAR and CoMFA analysis, it had been predicted that a hydrophilic inhibitor would bind in a distinctly different orientation than a hydrophobic inhibitor.^{23,24} Clearly this is not the case.

Given that previous structure–activity studies suggest that the ring nitrogen of the THIQ/THBA inhibitors mimics the β -hydroxyl group of the phenylethanolamine substrate,³¹ it is likely that phenylethanolamine sub-

strates would bind in such a manner that Val53 and Lys57 would interact with substituents on the aromatic ring. The β -hydroxyl group has been shown to be vital for methylation to take place,^{2,12,34–36} although there are some examples of methylation of conformationally defined phenylethylamines lacking the side chain hydroxyl.^{36,37} It is likely that the correct orientation of the substrate will be achieved through the interaction of the β -hydroxyl group with Glu219 and Asp267, and, furthermore, it is conceivable that Glu219 may play a role in activating the aliphatic amine for its nucleophilic attack on **3**.²⁶

To assess the relative importance of the residues contributing to both substrate binding and the recognition of the THBA and THIQ inhibitors, we replaced, in turn, each of Val53, Lys57, Glu219, and Asp267 with

Table 3. Kinetic Parameters for the hPNMT Catalyzed Methylation of Phenylethanolamine^a

hPNMT variant	α	3 (μM)		10 (μM)		k_{cat} (min^{-1})
		K_{d}	K_{m}	K_{d}	K_{m}	
WT	0.56	6.1 ± 0.4	3.4 ± 0.2	180 ± 8	100 ± 4	2.84 ± 0.10
V53A	1.35	7.1 ± 0.5	9.6 ± 0.7	1200 ± 120	1630 ± 170	3.40 ± 0.38
K57A	1.09	10.7 ± 2.2	11.7 ± 2.4	1200 ± 7	1310 ± 10	3.95 ± 0.67
E219A	0.95	7.5 ± 0.8	7.1 ± 0.8	610 ± 80	580 ± 76	1.31 ± 0.11
D267A	1.01	8.1 ± 0.7	8.3 ± 0.7	2010 ± 125	2050 ± 130	0.13 ± 0.02
D267N	0.95	7.5 ± 0.8	7.1 ± 0.8	1725 ± 70	1640 ± 70	0.10 ± 0.01

^a Initial rate data, obtained as described in Experimental Procedures, were fit to eq 1. Each data point is an average of at least three individual measurements, and values are reported as \pm SEM. The significance of K_{d} , K_{m} , and α are discussed in the Experimental Section.

alanine. In addition, Asp267 was also replaced with asparagine.

Contribution of Mutated Residues to Substrate Binding and Catalysis. The kinetic constants of the C-terminally 6X-histidine tagged hPNMT enzyme have been reported previously^{32,38} to be essentially identical to those obtained from the untagged enzyme. The WT-his₆ variant (hereafter referred to as WT) can be rapidly purified, and, consequently, the mutants were prepared as his₆-tagged variants. All mutants were routinely expressed and purified by affinity followed by size-exclusion chromatography as described previously.^{32,38} The circular dichroism spectra of WT hPNMT, and the mutants were essentially identical, indicating that the mutations had not resulted in any gross changes in secondary structure (data not shown). Of course, small localized changes in conformation cannot be ruled out.

The kinetic constants for WT hPNMT and all mutants are listed in Table 3. In line with previous observations,³⁸ the WT-enzyme was found to operate by a sequential mechanism with K_{m} values of 3.4 and 100 μM for **3** and phenylethanolamine (**10**), respectively. The K_{m} values are lower than the corresponding values of K_{d} , the dissociation constant for the hPNMT·substrate binary complex (which provides a measure of the substrate binding affinity). This indicates that there is synergy with substrate binding, i.e., the binding of the first substrate makes it easier for the second to bind and is characterized by an α value (eq 1) of less than unity.³⁹ None of the mutants showed any significant change in K_{d} for **3** which is consistent with the mutations all being located at some distance from its binding site. Conversely, all variants showed a decreased affinity for **10**, with increases in K_{d} ranging from 3-fold (E219A) to 10-fold (D267A). Although, under the conditions employed, there was no evidence for any change of mechanism, all mutations led to a loss of synergism of substrate binding; therefore, increases in the value of K_{m} were comparatively greater than the increases in K_{d} .

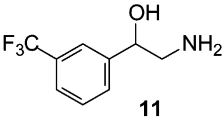
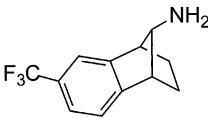
Only the mutations in Asp267 had a significant effect on k_{cat} values. Replacement of Asp267 by alanine resulted in a 20-fold decrease in k_{cat} , while replacement by the uncharged, but isosteric, asparagine resulted in a 28-fold decrease. Both variants showed similar decreases in substrate binding affinity. Given that asparagine can still act as a hydrogen bond acceptor these results suggest that it is the negative charge of Asp267 that is contributing to catalysis. Inspection of the hPNMT active site reveals that Asp267 forms an ion pair with Arg44 (Figure 3) and together these two residues form part of the "floor" of the phenylethanolamine/inhibitor binding site.^{26,27} It is not unreasonable

to suggest that disruption of the ion pair could adversely affect the active site geometry resulting in greater than expected reductions in both substrate and inhibitor binding affinity and, potentially, catalysis. However, preliminary indications are that, unlike Asp267, mutation of Arg44 has very little effect on catalytic rate (data not shown) so an alternative explanation was sought.

Since it is unlikely that the β -hydroxyl group of **10** will directly participate in the catalytic reaction, its principal role may be to interact with the enzyme so as to correctly position the flexible side-chain for nucleophilic attack on **3**. In a model of **1** bound to hPNMT, it was proposed that the β -OH group would interact with both Glu219 and Asp267.²⁶ If, as alluded to earlier, the interaction with Asp267 played a major role in substrate alignment, and therefore catalysis, it is certainly feasible that removal of that interaction would lower the value of k_{cat} . To examine this further the steady-state kinetics of 3-trifluoromethylphenylethanolamine (**11**) and a rigid analogue lacking the side chain hydroxyl group, *anti*-9-amino-6-(trifluoromethyl)benzonorbornene (**12**),³⁷ were determined with both WT and D267A. The data shown in Table 4 indicate that both **11** and **12** bind much more tightly to the WT enzyme than **10**, and that the D267A mutation considerably reduces the binding affinity for both these substrates. However, and most importantly, in marked contrast to the results for both **10** and **11** the k_{cat} values for **12** with both WT and D267A were quite similar. This shows that the lower k_{cat} values of the D267A variant observed with **10** and **11** are not due to an inherently reduced ability of this mutant to catalyze methyl transfer. Clearly the interaction of the β -OH group with the ionized side chain of Asp267 is important for catalysis by hPNMT and, apparently, is more important than its interaction with Glu219. Further, in the postulated model of **1** binding to hPNMT, it was proposed that the amine would interact with Glu219²⁶ and that Glu219 may act as a catalytic base facilitating methyl group transfer from **3**. The marginal decrease in value of k_{cat} for the E219A variant would seem to eliminate this possibility.

Contribution of Mutated Residues to Inhibitor Binding. The data for inhibitors binding to hPNMT and its variants are provided in Table 5. These data were obtained using a recently revised radiochemical assay⁴⁰ by varying the concentration of inhibitor and **10** at a fixed concentration of **3** (5 μM). In general, the assays were carried out at an enzyme concentration of 20 nM except for D267A which has a greatly diminished value of k_{cat} and required a concentration of 750 nM to obtain good kinetic data. In some cases, for the more potent inhibitors such as **7** and **9**, less enzyme (4 nM) was used, and, when the K_{i} value of the inhibitor was similar to

Table 4. Kinetic Data for **11** and Its Phenylethanolamine Analogue **12**^a

	WT	D267A
 <p style="text-align: center;">11</p>		
k_{cat} (min ⁻¹)	0.50 ± 0.01	0.06 ± 0.01
K_m 11 (μM)	0.55 ± 0.08	55 ± 12
K_d 11 (μM)	2.4 ± 0.7	265 ± 66
K_m 3 (μM)	1.2 ± 0.8	2.40 ± 0.8
K_d 3 (μM)	4.8 ± 0.5	11 ± 2
 <p style="text-align: center;">12</p>		
k_{cat} (min ⁻¹)	0.37 ± 0.04	0.26 ± 0.01
K_m 12 (μM)	1.5 ± 0.2	25 ± 1
K_d 12 (μM)	4.4 ± 1.0	66 ± 17
K_m 3 (μM)	2.0 ± 0.3	5.1 ± 1.2
K_d 3 (μM)	5.9 ± 1.5	13 ± 1

^a Initial rate data, obtained as described in Experimental Procedures, were fit to eq 1. Each data point is an average of at least three individual measurements and values are reported as ±SEM.

Table 5. In Vitro Inhibition Constants for hPNMT Variants^a

	7 K_i (nM)	8 K_i (μM)	9 K_i (nM)	13 K_i (μM)
WT-his	1.55 ± 0.21 ^{b,c}	0.12 ± 0.02	4.4 ± 1.1 ^{b,c}	0.04 ± 0.01 ^c
V53A	19.0 ± 2.0	0.62 ± 0.07	22.5 ± 2.1 ^c	0.13 ± 0.02
K57A	26.5 ± 3.5 ^c	6.9 ± 0.1	90.6 ± 4.7	0.74 ± 0.27
E219A	1375 ± 61	189 ± 20	3120 ± 270	17.9 ± 2.1
D267A ^d	999 ± 22 ^c	321 ± 13	590 ± 22 ^c	67.0 ± 6.1

^a All inhibition data were obtained at fixed concentration of **3** (5 μM) as described in Experimental Procedures. Unless stated otherwise, a hPNMT concentration of 20 nM was used, the data fitted to eq 2 and reported as ±SEM. ^b Obtained at an enzyme concentration of 4 nM. ^c Treated as a tight-binding inhibitor as described in the Experimental Section. ^d Obtained using an enzyme concentration of 750 nM.

the enzyme concentration, the inhibitors were treated as tight-binding.^{41,42} For all variants, each of the inhibitors was found to be competitive with respect to **10**, and the K_i values for **7–9** with WT hPNMT are in broad agreement with those obtained earlier using PNMT from various mammalian adrenal tissues.^{16,19,20,40} The K_i values previously reported for 7-iodo-THIQ (**13**)²⁷ and 7-nitro-THIQ (**14**)²⁴ are higher than those in Table 5 but were obtained using bovine PNMT and a different protocol. The lower values of K_i observed when assayed

under the conditions described herein are consistent with results for other similar compounds.⁴⁰

All mutations resulted in decreased binding affinity for each of the inhibitors. For the V53A variant, K_i values increased approximately 5 to 10-fold, i.e., comparable to the increase in the value of K_d for **10** and consistent with the structural evidence that the substituents on the aromatic ring of the inhibitors form favorable interactions with this residue. The effect of the K57A mutation was slightly greater than that of V53A with 20-fold decreases in binding affinity for all inhibitors except **8** whose K_i value increased almost 60-fold. The H-bonding interaction between the sulfonamide oxygens and the ε-NH₂ of Lys57 is expected to be 3–4 kcal/mol stronger than the van der Waals interactions between the ε-NH₂ and the halogen substituents on the other inhibitors (Table 2). It is likely that the greater increase in K_i value for **8** with K57A merely reflects the loss of the more favorable interaction. Presumably, replacement of either Val53 or Lys57 by alanine will create a larger binding pocket that no longer presents a complementary fit to the substrate/inhibitors.

Replacement of Glu219 with alanine led to a loss of synergy, but only a 6-fold increase in the value of K_d for **10**. By contrast the K_i values of the inhibitors increased by 2–3 orders of magnitude with **8** showing the largest increase, almost 1600-fold. Clearly Glu219 is much more important for the binding of inhibitors than it is for the phenylethanolamine substrates.

Once again the D267A variant provided the most puzzling results. Figure 3 shows that Asp267 has a direct interaction with **9**, rather than the water-mediated interactions observed for **7**, **8**, and **13**. The interatomic distances (Table 2) also suggest that **9** will have a stronger interaction with Asp267 than Glu219. Consequently, it would not be unreasonable to predict that replacement of Asp267 with alanine would have its greatest effect on the K_i value for **9**. In fact, as can be seen from Table 5, the reverse is true with the K_i value increasing only 135-fold which was 5-fold less for the E219A variant. While this increase is considerably greater than those observed for the V53A and K57A mutants, the D267A mutation affects the K_i values of **7**, **8**, and **13** much more adversely with increases ranging from 650-fold for **7** to more than 2650-fold for **8**. Conversely, the increase in the K_d value of the substrate, **10**, with the D267A variant was not greatly different from the increases in the K_d value of **10** with V53A and K57A.

While it is hard to rationalize the results for E219A and D267A with **9**, possibly of more import was that, with both these variants, the K_i values for all of the inhibitors increased by at least 2 orders of magnitude. This implies that the interaction between the amine of the inhibitors and the two carboxylic acid residues is stronger than their putative interaction with the β-hydroxyl group of the substrate. Presumably the latter interaction would be via a hydrogen bond whereas the THIQ interaction could potentially occur through ion-pair formation. These data support the notion that, at least for Glu219 where there is a direct interaction with the THIQ nitrogen, an ion-pair may form between the carboxylate and the amine. That said, previous results

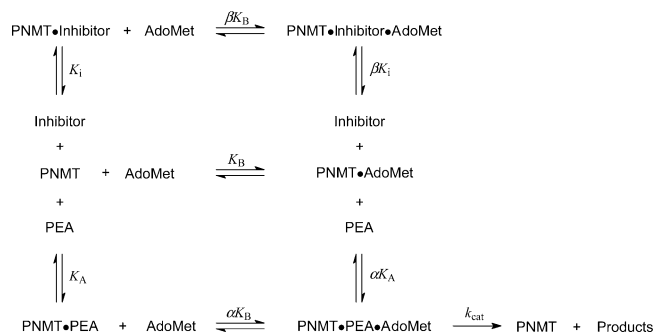


Figure 4. Equilibria describing a bireactant system for hPNMT wherein an inhibitor (I) competes with **10** (PEA, A) but allows **3** (AdoMet, B) to bind. The ternary complex (PNMT·Inhibitor·**3**) is inactive. The terms α and β are discussed in the text.

have indicated that THIQs and benzylamines bind to PNMT in their neutral form^{14,43} making ion-pair formation seem unlikely. Unfortunately, to date, there are no published structures of PNMT with a bound substrate that could help clarify the situation.

Preferential Binding of Inhibitor to the hPNMT·3** Complex.** One of the more intriguing aspects of catalysis by PNMT is the role of conformational changes in substrate/inhibitor binding. The X-ray structures clearly show that the binding sites for both substrates are enclosed by a tight cover, and it would seem that a conformational change will be required for access to the active site.²⁶ In this respect PNMT is similar to some other small molecule methyltransferases such as glycine *N*-methyltransferase^{44,45} and guanidinoacetate *N*-methyltransferase.³⁰ Earlier studies, as well as this work, have shown that THIQ¹⁶ and THBA¹⁹ inhibitors, as well as the benzylamines¹⁴ and amphetamines,¹³ bind competitively with respect to phenylethanolamine substrates. Historically the analysis of PNMT inhibition has been carried out at a fixed concentration of **3**. While obviously this provides information on the overall binding of the inhibitor to the enzyme, it does not specify whether the inhibitor binds to the free enzyme or to the PNMT·**3** complex (Figure 4). Synergism in substrate binding, as reflected in an α value of less than unity,³⁹ is often indicative of a conformational change occurring after the binding of either substrate.^{46,47} Given that hPNMT shows some synergism in substrate binding it is conceivable that a similar effect could occur for inhibitor binding. This can be examined by measuring the rate of reaction in the presence of varying amounts of inhibitor as the concentration of **3** and **10** are both varied.³⁹ Initially **8** was chosen for examination as it binds well to hPNMT but not so well as to require treatment as a tight-binding inhibitor (Table 5). Initial rate data were collected, fitted to eq 5 and the results shown in Table 6. The values (not shown) of K_m , K_d , and α for **3** and **10** determined in this experiment are in accord with those obtained for WT hPNMT shown in Table 3, underlining the internal consistency of the results. Like the α value for substrate binding, the value of β (eq 5) represents the factor by which the inhibitor dissociation constant is changed by the binding of, in this case, **3**. For **8**, the observed β value of 0.02 indicates that the inhibitor prefers to bind to the enzyme·**3** complex, rather than the free enzyme, by a factor of 50! This strongly supports the notion that the binding of **3**

Table 6. Inhibition Constants for Binding to Free hPNMT and to the hPNMT·**3** Complex^a

compound	K_i (μM)	β	βK_i (nM)	K_i^* (nM) ^b
5	1.33 ± 0.16	0.055 ± 0.007	72	121 ± 7
6	14.8 ± 2.1	0.154 ± 0.013	2270	3640 ± 240
8	2.84 ± 0.19	0.020 ± 0.001	57	120 ± 20
14	2.36 ± 0.54	0.024 ± 0.001	56	78 ± 14

^a Initial rate data were obtained as the concentrations of **3**, **10**, and inhibitor were each varied. These data were then fitted to eq 5 as described in experimental procedures. Values are reported as \pm SEM. The K_i value characterizes the binding of the inhibitor to free hPNMT while the value of βK_i characterizes the binding of the inhibitor to the hPNMT·**3** complex. ^b K_i^* values were obtained by varying the concentrations of **10** and inhibitor at fixed concentration of **3** ($5 \mu\text{M}$) and fitting initial rate data to eq 2.

brings about a conformational change in hPNMT. Furthermore, it appears that the conformational change is much more favorable to the binding of **8** than to the binding of the substrate, **10**. However, there should be one note of caution. While these data appear to be relatively clear-cut, it must be recognized that kinetic parameters do not always correlate with thermodynamic parameters, and it will be of interest to duplicate these results using a more direct measurement of substrate/inhibitor binding, such as isothermal titration calorimetry.

That said, these results are not without precedent as the binding affinity of oxamate, a competitive inhibitor of lactate dehydrogenase, increases 20-fold in the presence of NADH.⁴⁸ Further, the binding of the inhibitor, glyphosate, to 5-enolpyruvylshikimate-3-phosphate synthase has been associated with both a strong synergy of shikimate-3-phosphate, i.e., substrate, binding as well as stabilization of a “closed” form of the enzyme.⁴⁹ Notwithstanding those observations, it was intriguing that the 50-fold synergy in inhibitor binding was much greater than the 2-fold synergy in substrate binding.

To explore the structural basis of the **3**-enhanced affinity, three other inhibitors were examined using the same methodology. In the standard inhibition assay, **5** bound to hPNMT with an affinity akin to that of **8**, whereas **14** bound marginally more tightly and **6** bound more weakly (Table 6). The β values for the two THIQ inhibitors were similar suggesting the conformational changes in hPNMT upon binding of **3** resulted in greater affinity for the THIQ nucleus, rather than the individual substituents. Although the β value of the benzylamine-type inhibitor, **5**, was about double those of the THIQ derivatives, it still bound almost 20-fold tighter to the hPNMT·**3** complex than to the free enzyme. On the other hand, the β value for **6**, 0.15, was much closer to the α value for **10** (0.56) perhaps indicating that the **3**-induced conformational changes had similar effects on the binding of phenylethylamines and phenylethanolamines.

One possible explanation is that, while the binding sites of the substrate, **10**, and the THIQ and THBA inhibitors are overlapping, they are not identical. The THIQ inhibitors were originally designed as conformationally restrained analogues of β -phenylethylamines.¹⁶ It was subsequently shown that a fully extended side-chain was necessary for inhibition by phenylethylamines,⁵⁰ confirming the more generally held view that THIQ and THBA are, in fact, constrained analogues of benzylamine.⁵¹ In addition, results with conformation-

ally restricted analogues of **10** have suggested a fully extended side chain is essential for catalytic activity.³⁶ More recently, transferred nuclear Overhauser effect (TRNOE) experiments were used to show that, in the absence of **3**, **6** binds to bovine PNMT in an extended conformation.⁵² It is not unreasonable to assume that this conformation mimics the conformation of PNMT substrates binding to the enzyme and, if so, it may be expected that **6** would exhibit a β value more like the α value of a substrate than the β value of a THIQ-based inhibitor. Conversely, **5** is likely to have a β value more similar to those of **8** and **14**.

The experimental results appear to bear out those predictions, with **5** binding to hPNMT 20-fold more tightly in the presence of **3**. The THIQ analogue of α -methylbenzylamine, 1-methyl-THIQ, was about 3-fold less potent than THIQ,⁵³ suggesting that there are at least some unfavorable steric interactions in the binding of **5**. Therefore, the marginal difference between the β values of **5** and THIQ inhibitors could be assigned to a combination of side chain flexibility in the former as well as steric effects due to its α -methyl group. The β value for **6**, on the other hand, was significantly larger than those of the THIQ inhibitors but still 3-fold less than the α value for **10**. It is not entirely clear why, if the side-chain adopts an extended conformation, that the binding of **6** is more enhanced than that of **10** when **3** binds to hPNMT. It is conceivable that there is a population of conformers of **6** in which the side-chain is in the gauche (folded) conformation. If the binding of that small population to the hPNMT·**3** complex was tighter than that of the population in the extended conformation, a lower than expected β value would be observed.

At this point the reason for the benzylamine-type (including THIQ and THBA) inhibitors binding so much more tightly to the hPNMT·**3** complex than to the free enzyme is not clear. The X-ray structures show that the aliphatic nitrogen has interactions with both Glu219 and Asp267, and we have shown in this study that replacement of either of these residues with alanine results in relatively small changes in the values of K_m but large increases in K_i values. Given that both mutations lead to a loss of synergy in substrate binding, it is possible that there may be a similar loss of synergy for inhibitor binding. That alone would lead to a 50-fold increase in the value of K_i .

It should be noted that these experiments demonstrate that care must be taken with choosing the appropriate concentrations of **3** for routine inhibition studies where only the concentration of **10** is varied. We have previously described some problems with early measurements of K_i values for, in particular, tight-binding PNMT inhibitors.⁴⁰ In an effort to balance the sensitivity of the assay with the need for low enzyme concentration we suggested that a **3** concentration of 5 μ M may be appropriate. Clearly the results here demonstrate that the K_i values of the benzylamine-type inhibitors will depend strongly on the concentration of **3** and that, ideally, the concentration of **3** in routine assays should be at a saturating level. However, given the constraints of the assay, a concentration of **3** of 20 μ M, i.e., about 6 times K_m , is probably a reasonable compromise.

In summary, the X-ray structures of the hPNMT·**3**·**7** and hPNMT·**3**·**8** complexes demonstrate that, despite QSAR/CoMFA predictions, the lipophilic THIQ inhibitor, **7**, binds in a similar conformation to its hydrophilic counterpart, **8**. Unlike **10**, a substrate whose binding is enhanced 2-fold, inhibitors bind up to 50-fold more tightly to the hPNMT·**3** complex, suggesting that **3** brings about a conformational change favoring inhibitor binding. The residues, Glu219 and Asp267 clearly play a more important role in the binding of benzylamine-type inhibitors than they do in the binding of phenylethanolamine substrates. Taken together, it is conceivable that the binding of **3**, with its accompanying conformational change, results in Glu219 and Asp267 being better positioned to interact with inhibitors. In addition, Asp267 has been shown to be important for the correct alignment of substrates for catalysis, presumably through its interaction with the side-chain hydroxyl of the phenylethanolamines. The structures of the hPNMT·**3** complex and hPNMT bound to a substrate, when available, will go a long way toward confirming these hypotheses.

Experimental Procedures

Materials. Restriction enzymes and dNTPs were from Promega or New England Biolabs. Pfu DNA polymerase was from Stratagene. The wild-type hPNMT expression plasmid, pET17PNMT-his, was available from an earlier study.³² Primers for mutagenesis were obtained through the University of Michigan DNA Synthesis Core Facility or were purchased from Integrated DNA Technologies. Isopropyl β -D-thiogalactopyranoside (IPTG) was from Gold Biotechnology while compounds **3**, **5**, and **10** were obtained through Sigma. [³H]-**3** (15 Ci/mmol) was from Moravsek Biochemicals or Amersham Biosciences. Compounds **7** and **8** were kindly provided by Smith Kline and French Laboratories, GlaxoSmithKline, Philadelphia, PA. Compounds **6**,⁵² **9**,⁵⁴ **11**,³⁶ **12**,³⁷ **13**,²⁴ and **14**⁵⁵ were available from previous studies as their hydrochloride salts. All other buffers and reagents were the highest grade commercially available.

Preparation of hPNMT Variants. The mutants were prepared using Pfu DNA polymerase and the QuikChange site-directed mutagenesis kit (Stratagene), using pET17PNMT-his³² as the DNA template. The forward primers used for the mutagenesis are shown below with the mutated codons underlined, with the lowercase letters indicating a base change from wild-type:

V53A: 5'-GAACGGCGcCGGGCCGTGGAAGCTGCGC-3'

K57A: 5'-GTCGGGCCaTGgGcGCTGCGCTGCTTGGCGCAG

E219A: 5'-CGGGCCCTcGAGGcGTCTGGTACC-3'

D267A: 5'-CTTCAGACAGGCGTAGcTGAcGTCAAGGGCG-TC-3'

D267N: 5'-CTTCAGACAGGCGTAaATGAcGTCAAGGGCGTC-3'

In addition to creating the K57A and E219A mutations, these primers introduced a silent mutation which resulted in gains of *Nco*I and *Ava*I restriction sites, respectively. Silent mutations led to additional *Aat*II restriction sites for the D267A and D267N mutations, while for V53A the mutations resulted in gains of a *Nar*I restriction site. Following mutagenesis the template DNA was removed by treatment with *Dpn*I, and the remaining PCR products were transformed into *Escherichia coli* strain JM109 (Promega). Single colonies were picked, and in each case their DNA was isolated and screened for the desired mutation using the appropriate restriction enzyme. The fidelity of the PCR amplification and the presence of the mutation were confirmed by sequencing. For expression the plasmids were transformed into *E. coli* strain BL21(DE3)-pLysS (Novagen).

Expression and Purification of hPNMT Variants. The transformed cells were grown in LB medium at 37 °C until OD₆₀₀ reached ~0.6–0.8. The cells were cooled to 28 °C, and protein expression was induced by the addition of 0.5 mM IPTG. The cells were grown for an additional 4 h at 30 °C prior to harvesting by centrifugation at 7000 rpm for 8 min at 4 °C, then resuspended in a buffer comprising 50 mM sodium phosphate and 300 mM NaCl, pH 8.0 (Buffer A), containing 10 mM imidazole. After sonication and centrifugation, the cleared lysate was loaded onto His-Select HC Nickel Affinity column (Sigma) which had been equilibrated with Buffer A containing 10 mM imidazole. The enzyme was eluted with Buffer A containing 250 mM imidazole. The fractions containing hPNMT-his were pooled and concentrated, then loaded onto a Sephacryl S-200 high-resolution column (Pharmacia). The column was eluted with PNMT storage buffer consisting of 20 mM Tris (pH 7.2)/15% glycerol/1mM EDTA/0.5 mM DTT, and the fractions containing hPNMT-his were pooled, concentrated, and stored at 4 °C. Identical procedures were adopted for the expression and purification of the hPNMT variants. Protein concentrations were determined using the Bradford assay⁵⁶ with bovine serum albumin serving as the standard.

X-ray Crystallography. Purified hPNMT was concentrated to 50–60 mg/mL in a buffer containing 20 mM Tris-HCl pH 7.2 and 1 mM EDTA. The inhibitor, **7** (40 mM), and **4** (2 mM) were added such that the final concentration of protein was 30–40 mg/mL. The enzyme was cocrystallized with these compounds by hanging drop vapor diffusion on 3M tape with 1 μL protein/ligand mixture plus 1 μL precipitant over 100 μL precipitant (0.6–0.8 M NH₄PO₄, 0.1 M Na citrate pH 5.3–5.8). Crystals of appropriate size (>0.25 × 0.25 × 0.25 mm) were cryoprotected with 25% glycerol and flash frozen in a gaseous stream at 100 K for data measurement. X-ray diffraction data were measured using a Rigaku FR-E copper rotating anode generator operating at 45 kV, 45 mA with Osmic Confocal Max-Flux optics (either HiRes2 or maxxscreen). A Cryo Industries CryoCool LN2 with NeverIce ND1259 was used for cryocrystallographic data measurement, and reflections were measured with an R-AXIS IV++ imaging plate area detector. Crystallographic data were processed using Crystal Clear (Rigaku Corporation, (c) 1997–2002), and phasing was carried out using CNS v1.1.⁵⁷ The structures were solved by difference Fourier methods using the structure of PNMT·**4**·**8** (PDB 1HNN²⁶) as the model. Model building was performed using O,⁵⁸ and the structures were refined using CNS v1.1.⁵⁷ Initial coordinates for **7** were generated using the Insight II 2000 (Accelrys) builder module. Topology and parameter files were then generated using PRODRG⁵⁹ or XPLO2D⁶⁰ and modified where necessary. The procedure used was to model and refine the structure of the protein first, followed by addition of bound water molecules, **4**, and finally the inhibitor. *R*-free analysis (10% of reflections) was used for cross-validation.⁶¹ Coordinates and structure factors have been deposited with the protein data bank with accession code 1YZ3.

Steady-State Enzyme Kinetics. A standard assay mixture contained potassium phosphate (50 mM, pH 8.0), **10** (200 μM), and **3** including [³H]-**3** (5 μM), in a total volume of 250 μL. For determination of kinetic constants, the concentrations of both **3** and **10** were varied between 0.3 and 3 × *K_m*. Following the addition of enzyme, the reactions were incubated at 30 °C for 30 min and then quenched by the addition of 0.5 M boric acid (500 μL, pH 10.0). Two milliliters of a mixture of toluene/isoamyl alcohol (7:3) was added, and the samples were vortexed for 30 s. The phases were separated by centrifugation, and an aliquot of the organic phase (1 mL) was removed and added to 5 mL of scintillation fluid (Cytoscint, ICN). The radioactivity was quantitated by liquid scintillation spectrometry. For all variants the concentration of enzyme used in the assays was chosen so that the reaction rate varied linearly with enzyme concentration, and that amount of product formed was linear with time.

On the basis of Lineweaver–Burk plots and fits to kinetic equations, it has been shown that hPNMT operates by a sequential mechanism.³⁸ Accordingly, initial velocity data were

fitted to eq 1³⁹ using SigmaPlot 8.0 with the Enzyme Kinetics module from Systat Software Inc. (Richmond, CA),

$$v = \frac{k_{\text{cat}}[E][A][B]}{\alpha K_A K_B + \alpha K_A [B] + \alpha K_B [A] + [A][B]} \quad (1)$$

where [A] and [B] are the substrate concentrations of **10** and **3**, respectively, *K_A* and *K_B* are the dissociation constants (*K_d*) for the hPNMT·**10** and hPNMT·**3** complexes, respectively, α*K_A* and α*K_B* are the dissociation constants (*K_m*) of **10** and **3**, respectively, from the hPNMT·**10**·**3** ternary complex. Thus, the term α quantifies how the binding of one substrate affects the binding of the other.

Determination of Inhibition Constants (*K_i* Values). For routine inhibition assays the concentration of **3** was maintained at 5 μM. The concentration of **10** was then varied between 0.4 and 2.5 × *K_m* while the inhibitor concentrations varied between 0.4 and 2.5 × *K_i*. Initial velocity data were then fitted to eq 2.³⁹

$$v = \frac{V_{\text{max}}[S]}{[S] + K_m \left(1 + \frac{[I]}{K_i}\right)} \quad (2)$$

In some cases the value of *K_i* was similar to the enzyme concentration used in the assay. In those cases the inhibitors were considered to be tight-binding,^{41,42} and the kinetic data were fit to eqs 3⁴² and 4⁴¹ using the competitive tight-binding inhibition routine in the Enzyme Kinetics module.

$$v = v_0 \frac{[E] - [I] - K_i^{\text{app}} + \sqrt{([E] - [I] - K_i^{\text{app}})^2 - 4[E]K_i^{\text{app}}}}{2[E]} \quad (3)$$

$$K_i^{\text{app}} = K_i \left(1 + \frac{[S]}{K_m}\right) \quad (4)$$

Here, *v*₀ and *v* are the reaction rates in the absence and presence of inhibitor, respectively, [E] is the total enzyme concentration, [I] is the inhibitor concentration, and *K_i*^{app} is the enzyme–inhibitor dissociation constant at a fixed concentration of substrate.

Determination of Inhibitor Binding to the Free Enzyme and to the Enzyme·3** Complex.** In this instance initial velocities were measured as both **3** and **10** were varied between 0.4 and 2.5 × *K_m* while the inhibitor concentrations were varied between 0.4 and 2.5 × *K_i*. The data were then fit to eq 5³⁹ using SigmaPlot 8.0.

$$v = \frac{k_{\text{cat}}[E] \frac{[A][B]}{\alpha K_A K_B}}{1 + \frac{[A]}{K_A} + \frac{[B]}{K_B} + \frac{[I]}{K_i} + \frac{[A][B]}{\alpha K_A K_B} + \frac{[I][B]}{\beta K_i K_B}} \quad (5)$$

Here [A], [B], and [I] are the concentrations of **10**, **3**, and the inhibitor, respectively. As shown in Figure 4, *K_A*, *K_B*, and *K_i* are the dissociation constants for **10**, **3**, and the inhibitor, respectively, from the free enzyme. Again α is a measure of how the binding of one substrate affects the binding of the other, while β represents the factor by which the inhibitor dissociation constant is changed by the binding of **3**.

Acknowledgment. We thank Brian DeSmet and Amanda Dyelle for assistance with mutagenesis experiments, and Jian Lu, Mitchell R. Seim, and Kevin R. Criscione for critical reading of the manuscript. This work was supported by the Australian Research Council and by the NIH (Grant HL 34193).

References

- (1) Kirshner, N.; Goodall, M. The formation of adrenaline from noradrenaline. *Biochim. Biophys. Acta* **1957**, *24*, 658–659.

- (2) Axelrod, J. Purification and properties of phenylethanolamine *N*-methyltransferase. *J. Biol. Chem.* **1962**, *237*, 1657–1660.
- (3) Vogt, M. The concentration of sympathin in different parts of the central nervous system in normal conditions and after the administration of drugs. *J. Physiol. London* **1954**, *123*, 451–481.
- (4) Fuller, R. W. *Epinephrine in the Central Nervous System*; Oxford University Press: New York, 1988; pp 366–369.
- (5) Saavedra, J. M.; Grobecker, H.; Axelrod, J. Adrenaline-forming enzyme in brainstem: Elevation in genetic and experimental hypertension. *Science* **1976**, *191*, 483–484.
- (6) Rothballer, A. B. The effects of catecholamines on the central nervous system. *Pharmacol. Rev.* **1959**, *11*, 494–547.
- (7) Goldstein, M.; Lew, J. Y.; Matsumoto, Y.; Hökfelt, T.; Fuxe, K. *Psychopharmacology: A Generation of Progress*; Raven Press: New York, 1978; pp 261–269.
- (8) Crowley, W. R.; Terry, L. C.; Johnson, M. D. Evidence for the involvement of central epinephrine systems in the regulation of luteinizing hormone, prolactin, and growth hormone release in female rats. *Endocrinology* **1982**, *110*, 1102–1107.
- (9) Burke, W. J.; Chung, H. D.; Strong, R.; Mattammal, M. B.; Marshall, G. L.; Nakra, R.; Grossberg, G. T.; Haring, J. H.; Joh, T. H. *Central Nervous System Disorders of Aging: Clinical Intervention and Research*; Raven Press: New York, 1988; pp 41–70.
- (10) Kennedy, B. P.; Bottiglieri, T.; Arning, E.; Ziegler, M. G.; Hansen, L. A.; Masliah, E. Elevated S-adenosylhomocysteine in Alzheimer brain: influence on methyltransferases and cognitive function. *J. Neural. Transm.* **2004**, *111*, 547–567.
- (11) Krakoff, L. R.; Axelrod, J. Inhibition of phenylethanolamine *N*-methyltransferase. *Biochem. Pharmacol.* **1967**, *16*, 1384–1386.
- (12) Fuller, R. W.; Hunt, J. M. Substrate specificity of phenethanolamine *N*-methyl transferase. *Biochem. Pharmacol.* **1965**, *14*, 1896–1897.
- (13) Fuller, R. W.; Mills, J.; Marsh, M. M. Inhibition of phenylethanolamine *N*-methyltransferase by ring-substituted α -methylphenethylamines (amphetamines). *J. Med. Chem.* **1971**, *14*, 322–325.
- (14) Fuller, R. W.; Molloy, B. B.; Day, W. A.; Roush, B. W.; Marsh, M. M. Inhibition of phenylethanolamine *N*-methyltransferase by benzylamines. 1. Structure–activity relationships. *J. Med. Chem.* **1973**, *16*, 101–106.
- (15) Fuller, R. W.; Roush, B. W.; Snoddy, H. D.; Molloy, B. B. Inhibition of phenylethanolamine *N*-methyltransferase by benzylamines. 2. In vitro and in vivo studies with 2,3-dichloro- α -methylbenzylamine. *J. Med. Chem.* **1973**, *16*, 106–109.
- (16) Bondinell, W. E.; Chapin, F. W.; Girard, G. R.; Kaiser, C.; Krog, A. J.; Pavloff, A. M.; Schwartz, M. S.; Silvestri, J. S.; Vaidya, P. D.; Lam, B. L.; Wellman, G. R.; Pendleton, R. G. Inhibitors of phenylethanolamine *N*-methyltransferase and epinephrine biosynthesis. 1. Chloro-substituted 1,2,3,4-tetrahydroisoquinolines. *J. Med. Chem.* **1980**, *23*, 506–511.
- (17) Pendleton, R. G.; Kaiser, C.; Gessner, G. Studies on adrenal phenylethanolamine *N*-methyltransferase (PNMT) with SK&F 64139, a selective inhibitor. *J. Pharmacol. Exp. Ther.* **1976**, *197*, 623–632.
- (18) Pendleton, R. G.; Gessner, G.; Weiner, G.; Jenkins, B.; Sawyer, J.; Bondinell, W.; Intoccia, A. Studies on SK&F 29661, an organ-specific inhibitor of phenylethanolamine *N*-methyltransferase. *J. Pharmacol. Exp. Ther.* **1979**, *208*, 24–30.
- (19) Fuller, R. W.; Hemrick-Luecke, S.; Toomey, R. E.; Horng, J. S.; Ruffolo, R. R., Jr.; Molloy, B. B. Properties of 8,9-dichloro-2,3,4,5-tetrahydro-1*H*-2-benzazepine, an inhibitor of norepinephrine *N*-methyltransferase. *Biochem. Pharmacol.* **1981**, *30*, 1345–1352.
- (20) Pendleton, R. G.; Gessner, G.; Sawyer, J. Comparison of the effects of SK&F 29661 and 64139 upon adrenal and cardiac catecholamines. *Eur. J. Pharmacol.* **1980**, *68*, 117–127.
- (21) Kennedy, B.; Elayan, H.; Ziegler, M. G. Glucocorticoid hypertension and nonadrenal phenylethanolamine *N*-methyltransferase. *Hypertension* **1993**, *21*, 415–419.
- (22) Grunewald, G. L.; Caldwell, T. M.; Li, Q.; Slavica, M.; Criscione, K. R.; Borchardt, R. T.; Wang, W. Synthesis and biochemical evaluation of 3-fluoromethyl-1,2,3,4-tetrahydroisoquinolines as selective inhibitors of phenylethanolamine *N*-methyltransferase versus the α_2 -adrenoceptor. *J. Med. Chem.* **1999**, *42*, 3588–3601.
- (23) Grunewald, G. L.; Caldwell, T. M.; Dahanukar, V. H.; Jalluri, R. K.; Criscione, K. R. Comparative molecular field analysis (CoMFA) models of phenylethanolamine *N*-methyltransferase (PNMT) and the α_2 -adrenoceptor: the development of new, highly selective inhibitors of PNMT. *Bioorg. Med. Chem. Lett.* **1999**, *9*, 481–486.
- (24) Grunewald, G. L.; Dahanukar, V. H.; Jalluri, R. K.; Criscione, K. R. Synthesis, biochemical evaluation, and classical and three-dimensional quantitative structure–activity relationship studies of 7-substituted-1,2,3,4-tetrahydroisoquinolines and their relative affinities toward phenylethanolamine *N*-methyltransferase and the α_2 -adrenoceptor. *J. Med. Chem.* **1999**, *42*, 118–134.
- (25) Caine, J. M.; Macreadie, I. G.; Grunewald, G. L.; McLeish, M. J. Recombinant human phenylethanolamine *N*-methyltransferase: overproduction in *Escherichia coli*, purification, and characterization. *Prot. Express. Purif.* **1996**, *8*, 160–166.
- (26) Martin, J. L.; Begun, J.; McLeish, M. J.; Caine, J. M.; Grunewald, G. L. Getting the adrenaline going: crystal structure of the adrenaline-synthesizing enzyme PNMT. *Structure* **2001**, *9*, 977–985.
- (27) McMillan, F. M.; Archbold, J.; McLeish, M. J.; Caine, J. M.; Criscione, K. R.; Grunewald, G. L.; Martin, J. L. Molecular recognition of sub-micromolar inhibitors by the epinephrine-synthesizing enzyme phenylethanolamine *N*-methyltransferase. *J. Med. Chem.* **2004**, *47*, 37–44.
- (28) Fu, Z.; Hu, Y.; Konishi, K.; Takata, Y.; Ogawa, H.; Gomi, T.; Fujioka, M.; Takusagawa, F. Crystal structure of glycine *N*-methyltransferase from rat liver. *Biochemistry* **1996**, *35*, 11985–11993.
- (29) Horton, J. R.; Sawada, K.; Nishibori, M.; Zhang, X.; Cheng, X. Two polymorphic forms of human histamine methyltransferase: structural, thermal, and kinetic comparisons. *Structure* **2001**, *9*, 837–849.
- (30) Komoto, J.; Yamada, T.; Takata, Y.; Konishi, K.; Ogawa, H.; Gomi, T.; Fujioka, M.; Takusagawa, F. Catalytic mechanism of guanidinoacetate methyltransferase: crystal structures of guanidinoacetate methyltransferase ternary complexes. *Biochemistry* **2004**, *43*, 14385–14394.
- (31) Grunewald, G. L.; Skjærbaek, N.; Monn, J. A. An active site model of phenylethanolamine *N*-methyltransferase using CoMFA. *Trends in QSAR & Molecular Modelling 92*; ESCOM Science Publishers B. V.: Leiden, 1993; pp 513–516.
- (32) Romero, F. A.; Vodonick, S. M.; Criscione, K. R.; McLeish, M. J.; Grunewald, G. L. Inhibitors of phenylethanolamine *N*-methyltransferase that are predicted to penetrate the blood-brain barrier: design, synthesis, and evaluation of 3-fluoromethyl-7-(*N*-substituted aminosulfonyl)-1,2,3,4-tetrahydroisoquinolines that possess low affinity toward the α_2 -adrenoceptor. *J. Med. Chem.* **2004**, *47*, 4483–4493.
- (33) Grunewald, G. L.; Romero, F. A.; Criscione, K. R. 3-Hydroxy-methyl-7-(*N*-substituted aminosulfonyl)-1,2,3,4-tetrahydroisoquinoline inhibitors of phenylethanolamine *N*-methyltransferase that display remarkable potency and selectivity. *J. Med. Chem.* **2005**, *48*, 134–140.
- (34) Fuller, R. W.; Warren, B. J.; Molloy, B. B. Substrate specificity of phenylethanolamine *N*-methyltransferase from rabbit adrenal. *Biochim. Biophys. Acta* **1970**, *222*, 210–212.
- (35) Hoffman, A. R.; Ciaranello, R. D.; Axelrod, J. Substrate and inhibitor kinetics of bovine phenylethanolamine *N*-methyltransferase. *Biochem. Pharm.* **1974**, *24*, 544–546.
- (36) Rafferty, M. F.; Grunewald, G. L. The remarkable substrate activity for phenylethanolamine *N*-methyltransferase of some conformationally defined phenylethylamines lacking a side-chain hydroxyl group. *Mol. Pharmacol.* **1982**, *22*, 127–132.
- (37) Grunewald, G. L.; Markovich, K. M.; Sall, D. J. Binding orientation of amphetamine and norfenfluramine analogues in the benzonorbornene and benzobicyclo[3.2.1]octane ring systems at the active site of phenylethanolamine *N*-methyltransferase (PNMT). *J. Med. Chem.* **1987**, *30*, 2191–2208.
- (38) Caine, J. M. Cloning, expression and characterization of human phenylethanolamine *N*-methyltransferase. Ph.D. Dissertation, 1998, Monash University, Melbourne, Australia.
- (39) Segel, I. H. *Enzyme Kinetics: Behavior and Analysis of Rapid Equilibrium and Steady-State Enzyme Systems*; Wiley-Interscience: New York, 1975.
- (40) Wu, Q.; Criscione, K. R.; Grunewald, G. L.; McLeish, M. J. Phenylethanolamine *N*-methyltransferase inhibition: reevaluation of kinetic data. *Bioorg. Med. Chem. Lett.* **2004**, *14*, 4217–4220.
- (41) Copeland, R. A. Tight Binding Inhibitors. *Enzymes Second Edition: A Practical Introduction to Structure, Mechanism and Data Analysis*; Wiley-VCH: New York, 2000; pp 305–317.
- (42) Williams, J. W.; Morrison, J. F. The kinetics of reversible tight-binding inhibition. *Methods Enzymol.* **1979**, *63*, 437–467.
- (43) Grunewald, G. L.; Caldwell, T. M.; Li, Q.; Criscione, K. R. Synthesis and evaluation of 3-trifluoromethyl-7-substituted-1,2,3,4-tetrahydroisoquinolines as selective inhibitors of phenylethanolamine *N*-methyltransferase versus the α_2 -adrenoceptor. *J. Med. Chem.* **1999**, *42*, 3315–3323.

- (44) Huang, Y.; Komoto, J.; Konishi, K.; Takata, Y.; Ogawa, H.; Gomi, T.; Fujioka, M.; Takusagawa, F. Mechanisms for auto-inhibition and forced product release in glycine *N*-methyltransferase: crystal structures of wild-type, mutant R175K and *S*-adenosyl-homocysteine-bound R175K enzymes. *J. Mol. Biol.* **2000**, *298*, 149–162.
- (45) Takata, Y.; Huang, Y.; Komoto, J.; Yamada, T.; Konishi, K.; Ogawa, H.; Gomi, T.; Fujioka, M.; Takusagawa, F. Catalytic mechanism of glycine *N*-methyltransferase. *Biochemistry* **2003**, *42*, 8394–8402.
- (46) Furter, R.; Furter-Graves, E. M.; Wallimann, T. Creatine kinase: the reactive cysteine is required for synergism but is nonessential for catalysis. *Biochemistry* **1993**, *32*, 7022–7029.
- (47) Krell, T.; Maclean, J.; Boam, D. J.; Cooper, A.; Resmini, M.; Brocklehurst, K.; Kelly, S. M.; Price, N. C.; Laphorn, A. J.; Coggins, J. R. Biochemical and X-ray crystallographic studies on shikimate kinase: the important structural role of the P-loop lysine. *Protein Sci.* **2001**, *10*, 1137–1149.
- (48) Lai, C. J.; Wu, J. C. A simple kinetic method for rapid mechanistic analysis of reversible enzyme inhibitors. *Assay Drug Dev. Technol.* **2003**, *1*, 527–535.
- (49) Du, W.; Liu, W. S.; Payne, D. J.; Doyle, M. L. Synergistic inhibitor binding to *Streptococcus pneumoniae* 5-enolpyruvylshikimate-3-phosphate synthase with both monovalent cations and substrate. *Biochemistry* **2000**, *39*, 10140–10146.
- (50) Grunewald, G. L.; Borchardt, R. T.; Rafferty, M. F.; Krass, P. Conformational preferences of amphetamine analogues for inhibition of phenylethanolamine *N*-methyltransferase. *Mol. Pharmacol.* **1981**, *20*, 377–381.
- (51) Fuller, R. W.; Hemrick-Luecke, S. K. Comparison of some conformationally rigid benzylamine analogues as substrates for rabbit lung *N*-methyltransferase. *Res. Commun. Chem. Pathol. Pharmacol.* **1980**, *30*, 401–408.
- (52) Grunewald, G. L.; Palanki, M. S. S.; Vander Velde, D. Use of transferred nuclear Overhauser effects to determine the conformation of 1-(3,4-dichlorophenyl)-2-aminopropane when bound to the active site of phenylethanolamine *N*-methyltransferase (PNMT). *Bioorg. Med. Chem. Lett.* **1992**, *2*, 1681–1684.
- (53) Grunewald, G. L.; Sall, D. J.; Monn, J. A. Conformational and steric aspects of the inhibition of phenylethanolamine *N*-methyltransferase by benzylamines. *J. Med. Chem.* **1988**, *31*, 433–444.
- (54) Grunewald, G. L.; Paradkar, V. M. A regioselective synthesis of 8,9-dichloro-2,3,4,5-tetrahydro-1*H*-2-benzazepine (LY134046), a potent phenylethanolamine *N*-methyltransferase inhibitor. *Bioorg. Med. Chem. Lett.* **1991**, *1*, 59–60.
- (55) Grunewald, G. L.; Dahanukar, V. H.; Caldwell, T. M.; Criscione, K. R. Examination of the role of the acidic hydrogen in imparting selectivity of 7-(aminosulfonyl)-1,2,3,4-tetrahydroisoquinoline (SK&F 29661) toward inhibition of phenylethanolamine *N*-methyltransferase vs the α_2 -adrenoceptor. *J. Med. Chem.* **1997**, *40*, 3997–4005.
- (56) Bradford, M. M. A rapid and sensitive method for the quantitation of microgram quantities of protein utilizing the principle of protein-dye binding. *Anal. Biochem.* **1976**, *72*, 248–254.
- (57) Brünger, A. T.; Adams, P. D.; Clore, G. M.; DeLano, W. L.; Gros, P.; Grosse-Kunstleve, R. W.; Jiang, J. S.; Kuszewski, J.; Nilges, M.; Pannu, N. S.; Read, R. J.; Rice, L. M.; Simonson, T.; Warren, G. L. Crystallography & NMR system: A new software suite for macromolecular structure determination. *Acta Crystallogr. Sect. D* **1998**, *54*, 905–921.
- (58) Jones, T. A.; Zou, J. Y.; Cowan, S. W.; Kjeldgaard, M. Improved methods for building protein models in electron density maps and the location of errors in these models. *Acta Crystallogr. Sect. A* **1991**, *47*, 110–119.
- (59) Schuettelkopf, A. W.; van Aalten, D. M. F. PRODRG: a tool for high-throughput crystallography of protein–ligand complexes. *Acta Crystallogr. Sect. D* **2004**, *60*, 1355–1363.
- (60) Kleywegt, G. J.; Jones, T. A. Databases in protein crystallography. *Acta Crystallogr. Sect. D* **1998**, *54*, 1119–1131.
- (61) Brünger, A. T. Free *R* value: a novel statistical quantity for assessing the accuracy of crystal structures. *Nature* **1992**, *355*, 472–475.
- (62) Kraulis, P. J. MOLSCRIPT: a program to produce both detailed and schematic plots of protein structures. *J. Appl. Crystallogr.* **1991**, *24*, 946–950.
- (63) Merritt, E. A.; Bacon, D. J. Raster3D: photorealistic molecular graphics. *Methods Enzymol.* **1997**, *277*, 505–524.

JM0505680